ELSEVIER

Journal of Power Sources 75 (1998) 214–222

JOURNAL OF POWER SOURCES

# Anodic performance and mechanism of mesophase-pitch-derived carbons in lithium ion batteries

Isao Mochida *, Cha-Hun Ku, Seong-Ho Yoon, Yozo Korai

*Institute of Advanced Material Study, Kyushu University, Kasuga, Fukuoka 816-8580, Japan*

Received 27 March 1998; accepted 29 April 1998

**Abstract**

The anodic performance of soft carbons prepared from synthetic mesophase pitches by heat-treatment at 500 to 1200°C are investigated in order to clarify their mechanism for the insertion of lithium ions. It is found that the insertion mechanism for soft carbon heat-treated at low temperatures is divided into the following three cases: (i) lithium ions partially charge transferred on the surface of hexagonal planes or in the unstacked carbon layers to be charged and discharged at 0.25 to 0.8 V (Type I); (ii) intercalated into carbon layers up to a higher stage to be charged and discharged at 0.0 to 0.25 V (Type II); (iii) inserted into the microspaces located at the edges of carbon clusters to be charged at 0.0 to 0.1 V and discharged at 0.8 to 2.0 V (Type III). Lithium ions of Types I and II are charged and discharged reversibly, hence, the capacity is stable with cycling. By contrast, the capacity of Type III ions decreases gradually with cycle number. The irreversible charge–discharge and poor cycle stability of Type III ions suggest some chemical reactions during charge–discharge that increase the discharge potential and modify the carbon structure. Bonding of carbon planes at facing edges in the anisotropic carbon may be responsible for the poor cycle stability. The capacity of Type II ions increases gradually with heat-treatment which graphitizes carbon to allow intercalation. By contrast, the capacities of Types I and III ions are decreased gradually and sharply, respectively, by heat-treatment. The progress of graphitization densifies the carbon and reduces the free surface of the hexagonal sheet and the charging to such sites. The performance of Type III ions reflects the characteristic of anisotropic carbon in which the clusters are aligned to have more faced edges than those in isotropic carbon. The heat-treatment combines the edges to enlarge considerably the hexagonal plane in this temperature range. 

*Keywords:* Anode materials; Carbon; Electrochemical behaviour; Lithium ion batteries

## 1. Introduction

Recently, the lithium-ion secondary battery has attracted considerable attention because of its high specific energy and power, long cycle life and safety, the last of which was the main problem with the lithium metal battery. It is well known that such performance is related intimately to the characteristics of the carbon materials which are used as the anodic materials. Therefore, extensive studies have been conducted on carbon materials for lithium-ion secondary batteries.

Many kinds of carbons prepared from different starting materials by means of various carbonization procedures have been tested to find the best anode for the lithium-ion secondary battery [1–8]. The carbons display different performances according to their structure or properties. The carbon materials are basically classified into the following three groups [2]: (i) graphitized carbon; (ii) some hard carbons heat-treated at 1000 to 1400°C; (iii) most soft carbons heat-treated at 600 to 800°C. The insertion mechanism of lithium ions into graphite is well known and is termed 'intercalation' [9,10]. By contrast, the mechanism for the other two types of carbons is not yet clear, although several models have been proposed [1,2,8,11–15].

Carbons heat-treated around 700°C exhibit quite different performance to that of graphite [1,5,8,11,13,16]. They yield larger capacity per weight than that of graphite by two or three times, although there are several disadvantages for commercial use such as high irreversible capacity, high de-insertion potential (i.e., low discharge voltage in practical cells) and poor cycle stability. They are of poor crystallinity and have small hexagonal planes. Hence, very

* Corresponding author. Tel.: +81-92-583 7797: Fax: +81-92-583 7798

0378-7753/98/$19.00 
PII: S0378-7753(98)00101-3

different kinds of lithium-insertion mechanism should be considered. To date, several mechanisms have been proposed in order to explain the lithium insertion mechanism into carbons of this type [1,2,5,8,11–15]. According to Tokumitsu et al. [8] and Mabuchi et al. [11], the capacity of carbons is ascribed to intercalation into hexagonal layers of partial crystallinity, and insertion into the cavity represented by the cavity index. Sato et al. [1] suggested the formation of $LiC_2$. Liu et al. [12] and Zheng et al. [13] proposed insertion of lithium into hydrogen-containing carbons to interact with hydrogen or to spaces among the cage of hexagonal carbon cards. However, these models are not sufficient to explain completely the performance of the carbon.

In this study, we have measured the performance of soft carbon calcined around 700°C to determine the possible mechanism for lithium insertion into not fully organized carbon. The mechanism should explain a set of performances consistently. Hence, it is first necessary to define how many sets of performance, and then to propose the mechanism to explain respective sets of performance by types of lithium insertion in the particular structure of the carbon.

## 2. Experimental

Mesophase pitches were synthesized from naphthalene (NP) and methylnaphthalene (mNP) using $HF/BF_3$ as a catalyst (supplied by Mitsubishi Gas Chemical). Table 1 shows the elemental analyses and some properties of the mesophase pitches.

### 2.1. Carbonization and calcination

The mesophase pitch was carbonized at 600°C for 30 min, and then further calcined at 700 to 1200°C for 1 h after grinding to pass 325-mesh screen. The mesophase pitch was carbonized through a liquid phase, and exhibited a large volume expansion at the final stage of the carbonization, to give anisotropic texture to the resultant coke. The heating rate was 10°C $min^{-1}$ for both carbonization and calcination.

### 2.2. Structure and properties

The structure of each carbon was estimated by elemental analysis and X-ray diffraction to obtain the H/C ratio, $d_{002}$, and $L_{c(002)}$.

The specific resistivity of each carbon electrode under charge–discharge tests was measured using the 4-terminal method. The density was measured by the butanol displacement method.

### 2.3. Electrochemical performance

Carbon electrodes were prepared by pressing on SUS mesh as a current-collector after mixing carbon with 10 wt.% PTFE (polytetrafluoroethylene) as a binder. It was dried at 200°C for 12 h under vacuum before measurement.

The electrochemical cell consisted of three electrodes, viz., carbon as the working electrode, lithium foil as the counter and the reference. Each cell was kept standing for 12 h after assemble in order to assure sufficient wetting of the active material with electrolyte (1 M $LiPF_6$/EC + DMC, vol. ratio 1:1).

A constant current of 0.2 mA $cm^{-2}$ was usually applied throughout the charge and discharge stages. The limited potential method, where the charge potential was maintained at given value (in this study zero volts) for a prescribed time (40 h), was also applied in order to obtain the maximum capacity.

## 3. Results

### 3.1. Structure and properties of carbons

Table 2 summarizes the structural factors of each carbon, as obtained from elemental analyses and X-ray diffraction. The hydrogen content is decreased drastically by heat-treatment between 600 and 700°C, and then gradually. Extensive heat-treatment at 600°C for 40 h hardly changes the hydrogen content, while longer heat-treatment at 700°C decreases the content considerably. Carbon heat-treated at 700°C for 10 h exhibits much the same amount

Table 1
Elemental analyses and properties of mesophase pitches

| Code | Starting material | AC (%)[a] | SP (°C)[b] | Elemental analyses | | | Solubility (%) | | | fa[c] |
|---|---|---|---|---|---|---|---|---|---|---|
| | | | | C | H | H/C | BS[d] | BI–PyS[e] | PyI[f] | |
| NA-MP | naphthalene | 100 | 237 | 94.58 | 5.09 | 0.65 | 46 | 21 | 33 | 0.94 |
| mNA-MP | methylnaphthalene | 100 | 227 | 94.13 | 5.31 | 0.68 | 41 | 27 | 32 | 0.94 |

[a]Anisotropic content.
[b]Softening point.
[c]Carbon aromaticity.
[d]Benzene soluble.
[e]Benzene insoluble–pyridine soluble.
[f]Pyridine insoluble.

Table 2
Some analytical properties of carbons prepared from NP and mNP mesophase pitches

| Code | HTT (°C) | Holding time (h) | Elemental analyses | | | XRD | |
|---|---|---|---|---|---|---|---|
| | | | C | H | H/C | $d_{002}$ (nm) | $L_{c(002)}$ (nm) |
| NP500 | 500 | 1 | 95.79 | 3.50 | 0.44 | 0.3460 | 2.4 |
| NP600-1 | | 1 | 95.41 | 2.99 | 0.38 | 0.3462 | 2.2 |
| NP600-10 | 600 | 10 | 96.01 | 2.72 | 0.34 | 0.3472 | 1.4 |
| NP600-20 | | 20 | 95.93 | 2.48 | 0.31 | 0.3470 | 1.4 |
| NP700-1 | | 1 | 97.15 | 1.50 | 0.19 | 0.3504 | 1.2 |
| NP700-5 | 700 | 5 | 97.74 | 1.17 | 0.14 | 0.3498 | 1.2 |
| NP700-10 | | 10 | 97.84 | 1.10 | 0.13 | 0.3494 | 1.2 |
| NP800 | 800 | 1 | 98.17 | 1.04 | 0.13 | 0.3494 | 1.4 |
| NP1000 | 1000 | 1 | 99.06 | 0.44 | 0.05 | 0.3489 | 2.7 |
| NP1200 | 1200 | 1 | 99.37 | 0.25 | 0.03 | 0.3488 | 3.8 |
| mNP600 | 600 | 1 | 95.47 | 2.90 | 0.36 | 0.3478 | 2.0 |
| mNP700 | 700 | 1 | 97.72 | 1.11 | 0.14 | 0.3504 | 1.3 |
| mNP1200 | 1200 | 1 | 99.25 | 0.14 | 0.02 | 0.3487 | 3.8 |

of hydrogen as carbon heat-treated at 800°C for only 1 h. The carbons prepared from mNP mesophase pitch have a relatively small hydrogen content, comparing with that from NP mesophase pitch.

No significant change is found in the XRD pattern up to 800°C although the graphitization of the carbon is improved. The carbon heat-treated at 600°C appeared to have higher crystallinity than those heat-treated at 700 to 800°C, but the average size of the hexagonal plane estimated from the hydrogen content is certainly smaller than those of NP700 and NP800 carbons. No major differences in the crystallographic parameters of the carbon are suggested, even if the layered stacking in the carbon precursor pitch is still maintained in this heat-treatment temperature (HTT) range.

Table 3 shows the specific resistivity and the density of the carbons. The specific resistivity of the carbon heat-treated at 600°C is still very high, but it decreases dramatically at 700°C. The changes in resistivity and hydrogen content are intimately correlated. The change in density is also similar to that of specific resistivity, although the change during 600 to 700°C is not so drastic. Extended heat-treatment at 600 and 700°C also changes both the specific resistivity and the density of the carbons.

Table 3
Properties of carbons prepared from NP mesophase pitch

| Code | Specific resistivity[a] (Ω cm) | Density[b] (g $cm^{-3}$) |
|---|---|---|
| NP600-1 | $>10^6$ | 1.39 |
| NP600-10 | $3\times10^5$ | 1.48 |
| NP600-20 | $1\times10^5$ | 1.54 |
| NP700-1 | 27 | 1.59 |
| NP700-5 | 11 | 1.69 |
| NP700-10 | 5.4 | 1.71 |
| NP800 | 2.7 | 1.79 |
| NP1000 | 0.9 | 1.94 |
| NP1200 | 0.6 | 1.96 |

[a] Measured by 4-terminal method.
[b] Butanol displacement density.

### 3.2. Charge–discharge characteristics of carbon anode

The charge–discharge characteristics measured by the constant-current method are presented in Fig. 1. As shown in Table 3, the electric conductivity of carbon heat-treated at 600°C for 1 h is very low, hence, charge–discharge tests were carried out on carbons heat-treated at 700 to 1200°C. Both charge and discharge capacities of such carbons decreased with the HTT. Several aspects of the charge profile varied strongly with the HTT. A short plateau at about 0.8 V, which may be ascribed to an irreversible reaction of the electrolyte on the carbon surface, decreased with HTT. The charge capacity at 0.0 to 0.25 V also decreased with HTT (Type II). By contrast, the potential profile (a monotonic decrease) at 0.25 to 0.8 V was much

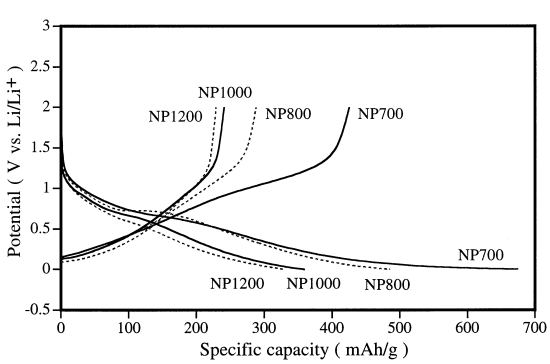


Fig. 1. Potential–capacity profiles for the first cycle of carbons prepared from NP mesophase pitch at various temperatures. Constant-current method of charging (0.2 mA $cm^{-2}$) over potential range 0.0 to 2.0 V.

the same regardless of the HTT (Type I), although slight increase in the capacity was observed. The increasing potential in the discharge profile over this region agreed with that of charge, i.e., showed no significant change with HTT, although the capacity slightly increased with HTT. The plateau at about 1 V in the discharge profile was increased considerably with increasing charge capacity below 0.1 V (Type III). The charge–discharge reaction at 0.0 to 0.25 V appeared to be reversible, although the capacity increased slightly with the HTT. These results of charge and discharge indicate at least three mechanisms of lithium insertion into carbons which are heat-treated below 1200°C.

Fig. 2 shows the charge–discharge profiles of representative carbons at different currents. It has been known that such profiles are affected mainly by the total impedance of the cell which includes contributions from the chemical reactions, the overpotential on the surface of carbon, the electric conductivity of the electrode, the ionic conductivity of the electrolyte and the diffusivity of lithium. The lower HTT enlarges effects of the charge–discharge rate on the performance. Therefore, the carbons heat-treated at 600 to 700°C do not show their maximum capacity under constant-current charge because the charge potential always shifts to a more negative value. Consequently, charging to the maximum capacity of each carbon is necessary in order to obtain a significant correlation between the electrochemical behaviour and the structure of the carbon.

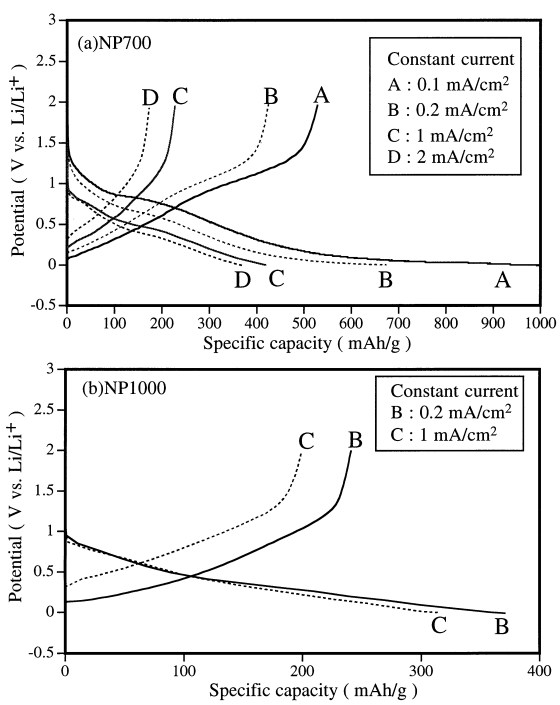


Fig. 2. Potential–capacity profiles for the first cycle of NP700 (a) and NP1000 (b) at various current densities.

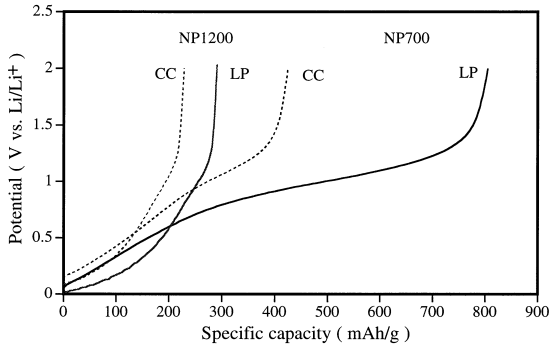


Fig. 3. Discharge profiles of carbons prepared from NP after charging by different methods: CC: constant-current method (0.2 mA $cm^{-2}$), LP: limited potential method (constant-current charge at 0.2 mA $cm^{-2}$ followed by constant-potential charge at 0 V for 40 h).

### 3.3. Comparison of charging procedures

Changes in the discharge characteristics caused by different charging methods are illustrated in Fig. 3. Under constant-potential charging at 0 V, the discharge capacity of NP700 (carbon from NP mesophase pitch carbonized at 700°C) becomes larger than that obtained by constant-current charging; the plateau at around 1 V is enlarged. By contrast, charging methods exert a much smaller influence on the capacity of NP1200 (carbon from NP mesophase pitch carbonized at 1200°C), although the limited potential method slightly increases the discharge capacity over the 0.0 to 0.25 V region.

### 3.4. Discharge characteristics of carbons heat-treated at 500 to 1200°C

Fig. 4 gives the discharge voltage profiles of carbon heat-treated at 500 to 1200°C for 1 h (NP500 to NP1200), in which the limited-potential charging method was applied. NP600 displayed the largest capacity, while NP500 yielded very little capacity regardless of the charging method.

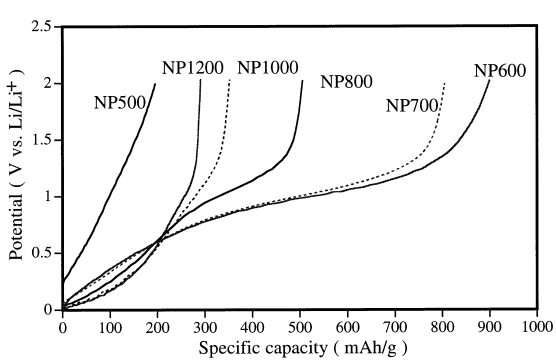


Fig. 4. Potential–capacity profiles for the first cycle of carbons prepared from NP charged by limited potential method (constant-current charge at 0.2 mA $cm^{-2}$ followed by constant-potential charge at 0 V for 40 h).

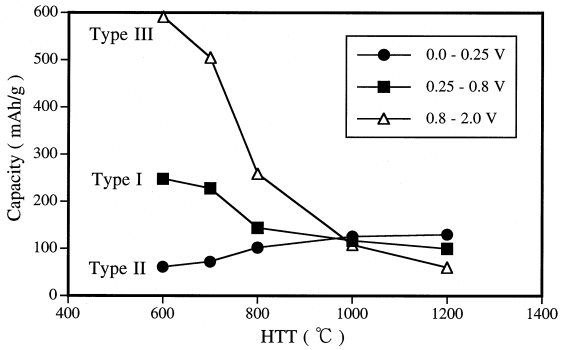


Fig. 5. Change of discharge capacity in divided potential range for first cycle of carbons prepared from NP heat-treated at various temperatures. The carbons were charged by the limited-potential method.

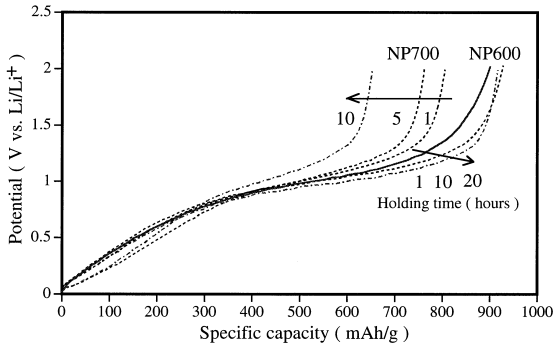


Fig. 7. Potential–capacity profiles for first cycle of carbons prepared from NP by heat-treatment for various periods. The carbons were charged by the limited-potential method.

The discharge capacity decreased with the increase in the HTT from 600 to 1200°C, reducing the discharge plateau at about 1 V, whereas the capacity below 0.25 V increased very slightly. Another major change in the discharge profile was observed at 0.0 to 0.5 V, namely, heat-treatment above 800°C provided a lower potential than heat-treatment below 800°C.

The discharge capacities over three potential ranges of carbons heat-treated at 600 to 1200°C are presented in Fig. 5. The discharge capacity exhibits very different responses to the HTT of the carbon. The discharge capacity of Type II increases very gradually with HTT, whereas that of Types I and III decreases with HTT moderately and very sharply, respectively. This suggests three different insertion mechanisms of lithium into three parts of the carbon.

The irreversible capacity and coulombic efficiency of the first cycle together with the reversible capacity are shown in Fig. 6 as a function of the HTT. The irreversible capacity of the first cycle, which has been ascribed to the reactions of electrolytes on the surface of carbons as well as lithium with some reactive sites in the carbon, decreases with increase in the HTT. Thus, the coulombic efficiency is very low with carbon heat-treated at 500°C, increases sharply with heat-treatment up to 600°C, stays rather constant up to 700°C, and then increases gradually to level off beyond 1000°C.

### *3.5. Influence of extended heat-treatment and carbon precursor on discharge performance*

The change in discharge characteristics of NP-carbons prepared by extended heat-treatment at 600 and 700°C is shown in Fig. 7. The capacity of NP600 increases at longer holding times by extending the plateau at 1 V, although that of NP700 decreases by reducing the plateau. It is noted that longer heat-treatment at 700°C changes the structure of the carbon, but not at 600°C.

A comparison of the discharge performance of mNP derived carbon (mNP) heat-treated at 600 and 700°C for 1 h is given in Fig. 8. NP and mNP carbons heat-treated at 600 and 700°C display much the same profile although the mNP carbon exhibits slightly larger and smaller capacities at a HTT of 600 and 700°C, respectively. There are no major differences in the performance of carbons heat-treated at 1200°C.

### *3.6. Cycle stability of representative carbons*

The cycle stability of NP-based carbons prepared at 600°C and 1000°C is shown in Fig. 9. The discharge

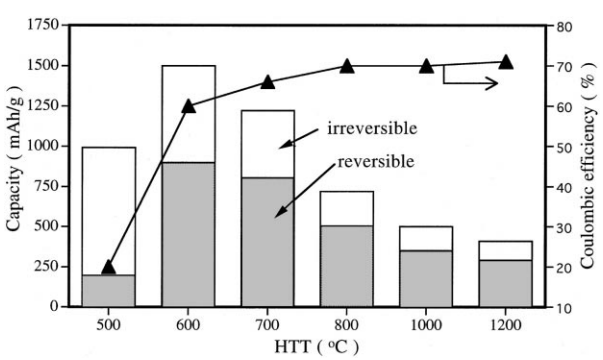


Fig. 6. Change of reversible capacity and coulombic efficiency for first cycle of carbons prepared from NP heat-treated at various temperatures. The carbons were charged by the limited-potential method.

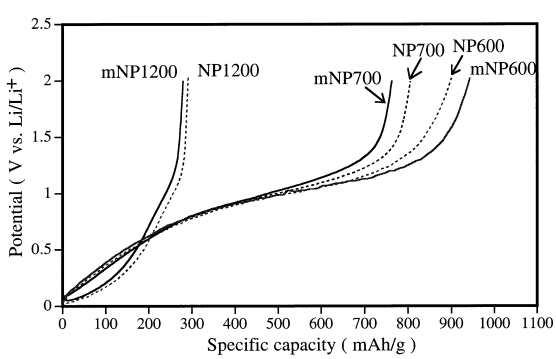


Fig. 8. Potential–capacity profiles for first cycle of carbons prepared from NP and mNP. The carbons were charged by the limited-potential method.

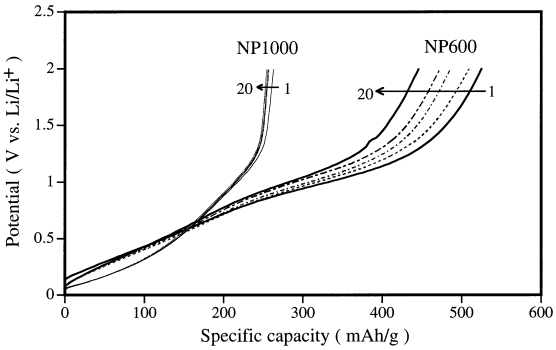


Fig. 9. Change of potential–capacity profile of carbons prepared from NP with cycle number (1 to 20). Constant-current charging method (0.2 mA $cm^{-2}$).

capacity of NP1000 decreases a little from the first to the third cycle in the potential region about 1.0 V, and then becomes very stable up to the 20th cycle. By contrast, the discharge capacity of NP600 decreases continuously up to 20th cycle. A major decrease is observed in the potential region about 1.0 V.

The cycle stability of the discharge capacity in the three potential ranges of carbon heat-treated at 600 and 1000°C is given in Fig. 10a and b, respectively. The capacity of NP600 at Types I (0.25 to 0.8 V) and II (0.0 to 0.25 V) is relatively stable with cycling, but the capacity at Type III (0.8 to 2.0 V) decreases very markedly. The capacity of NP1000 is much more stable although the capacity at Type III decreases a little on the first cycle and then becomes stable.

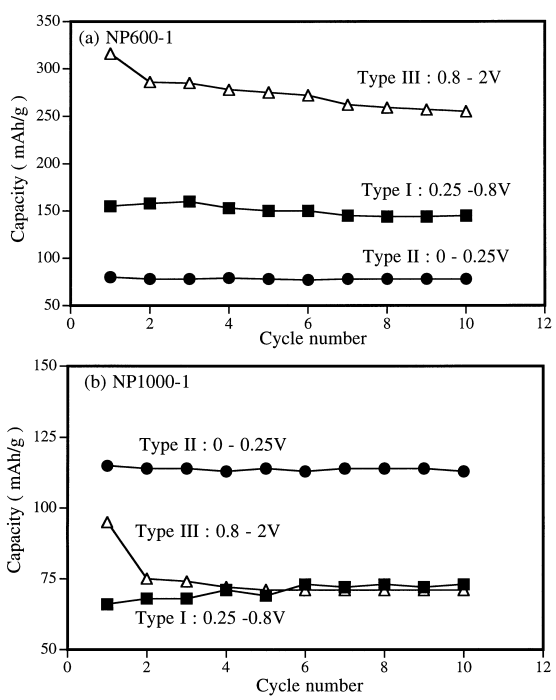


Fig. 10. Cycle stability of (a) NP600-1 and (b) NP1000-1 in the divided potential range. The carbons were charged and discharged by the constant-current method (0.2 mA $cm^{-2}$).

### 3.7. Correlations between anodic performance and structural parameters of carbons

An attempt has been made to correlate the capacity, classified into three types, with some structural parameters of the carbon that vary with the HTT and the precursors. The capacity at Type II (0 to 0.25 V) is correlated with the $L_{c(002)}$ of the carbon in Fig. 11a. The $L_c$ value decreases at first with heat-treatment at 500 to 700°C and longer soak times and then increases monotonously above 800°C. Lithium ions in this region appear to be inserted into the stacked layers of carbon heat-treated above 1000°C as higher stage intercalation. Higher stacking allows larger capacity of Type II. Highly reduced lithium gets into the interspace of the carbon and is discharged almost reversibly. By contrast, the carbons heat-treated at 500 to 600°C yield very small capacity for this type, even though they appear to have higher stacking than that of NP700. The stacking of mesophase aromatic rings to hexagonal carbon sheet may take place in this HTT region. Not only high stacking but also large hexagonal planes may be indispensable for intercalation up to higher stage.

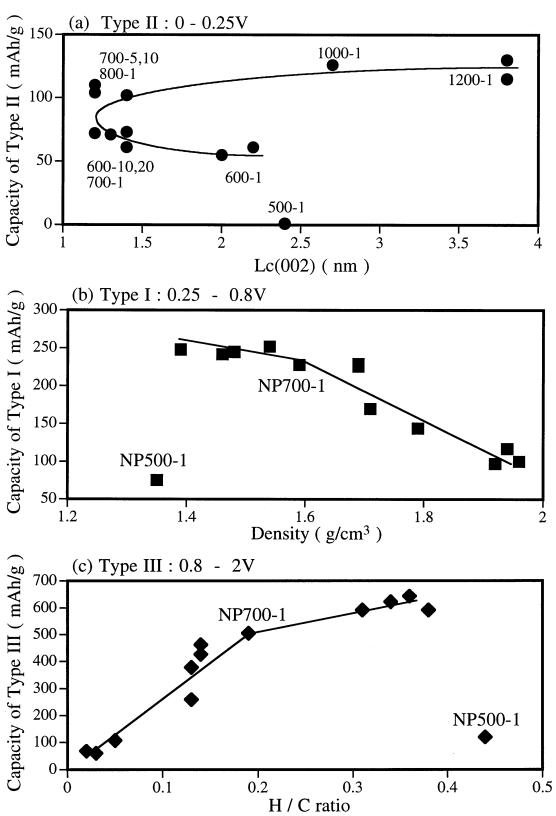


Fig. 11. Correlation between reversible capacity divided into three potential regions and structural factors of carbons prepared from NP and mNP. (a) Capacity of Type II vs. $L_{c(002)}$; (b) Type I vs. density; (c) Type III vs. H/C ratio. Limited-potential charging method.

Charge transfer of partially-reduced lithium ions may occur very reversibly to the hexagonal plane or in the disordered carbon plane over a wide potential range during the charge procedure. Type I indicates this kind of charge–discharge. The capacity is correlated to the density of carbon in two regions, as shown in Fig. 11b. The high resistivity of carbons heat-treated below 700°C may disturb the charge as indicated by the low capacity of NP500-1. Maximum capacity cannot be accomplished even with constant-potential charging for 40 h. The density may be related to the stacking order, hence, higher density reduces the surface of free hexagonal planes.

The capacity of Type III is well correlated with the H/C ratio or the hydrogen content, and is divided into two regions, as shown in Fig. 11c. The capacity is charged at 0 to 0.1 V and discharged at about 1 V, and exhibits very poor cycle stability. Therefore, certain chemical reactions are assumed to take place during charging at about 0 V. This reaction may be due to hydrogen on the edge of hexagonal plane causing an irreversible change in the carbon structure. Most of the hydrogen is expected to exist as an aromatic type at the periphery of the hexagon in the carbons heat-treated above 600°C as indicated by $^{13}$C-NMR. Thus, it is noted that the hydrogen content may indicate the amount of microspace at the edge-to-edge of the clusters. Although all the hydrogen may not behave in the same manner, the hydrogen content is well correlated to the reversible capacity of Type III, as shown in Fig. 11c.

The correlation between undischargeable charging capacity for the first cycle charged with constant-potential charging for 40 h and the H/C ratio is given in Fig. 12. The undischargeable capacity is obtained by substrating the discharge capacity at 0.8 to 2.0 V from the capacity charged during the constant-potential range. These values are measured on the second cycle in order to include other irreversible capacity which occurs on the first cycle. This capacity reflects the chemical reactions of lithium charged at 0.0 to 0.1 V and also corresponds to the difference between the capacity for constant-potential charge for 40 h and the discharge capacity. Part of these lithium ions is discharged at about 1 V to cause a change in the carbon structure, while another part reacts with hydrogen on the carbon edges to be oxidized or not to be discharged.

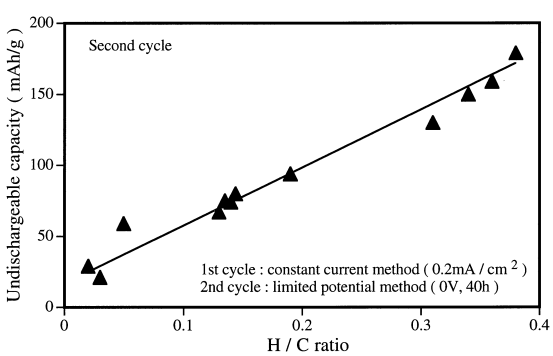


Fig. 12. Correlation between undischargeable capacity and H/C ratio for carbons charged by the constant-potential method at 0 V for 40 h.

## 4. Discussion

In the present study, the anodic performance of a series of carbons derived from synthetic mesophase pitches by means of heat-treatment at 500 to 1200°C is correlated with carbon structural factors. The performance in question includes the discharge capacity, the potentials of charge and discharge, the undischargeable charge, and the reactivity of the electrolyte in the presence of low-valent lithium on the carbon surface. Such parameters vary with the cycle number, which indicates that the carbon may change its structure during charge–discharge cycling through reactivity with low-valent lithium.

First of all, the dischargeable capacity of the present series of carbons is classified into three categories according to the charge and discharge potentials, cycle stability and influence of the HTT. Each category has its own mechanism and site of the lithium insertion. The mechanisms so far proposed appear to neglect the fact that carbon exhibits different charge and discharge behaviour according to the charging method and starting material.

The discharge capacity at 0 to 0.8 V is stable with cycling and appears common to all carbons; it depends slightly on the HTT and the starting pitch except for 500°C. This capacity is basically discharged at the same potential as that of charge. Such performance indicates the reversible charge-transfer of partly reduced lithium ions to the carbon plane (Type I) and intercalation into the stacked layer to the higher stage (Type II), even though the stacking height is still small. The capacity of Type I is related to the density of the carbon which may be a parameter for the quantity of the free hexagonal surface. The charge and discharge potential profiles of this region are different in shape according to the HTT.

Heat-treatment at high temperatures allows more discharge at lower potential as classified by Type II. Growth of stacking in terms of both $L_{c(002)}$ and $d_{(002)}$ may require a lower valence of lithium to overcome the energy necessary for the widening of the interlayer space and reduce the surface of the stacking. The intercalation nature of the higher stage is more emphasized in the carbon heat-treated at temperatures above 800°C (Type II) rather than the simple charge-transfer to the hexagonal plane that is observed with the carbon of least stacking heat-treated at lower temperatures (Type I). Such charge–discharge is reversible and, as it causes no structural change of the carbon, is stable with cycling.

The third part of discharge is obtained by charging at a low potential of below 0.1 V and is very much dependent upon the HTT and the time, kinds of pitch, and cycle number. The major portion of the discharge decreases with charge–discharge cycling. Charging at lower potential and

discharge at higher potential are characteristic of anisotropic carbons calcined at low temperature (Type III). Long heat-treatment at 600°C increases the capacity of this type, while higher temperature reduces the capacity. The capacity of this type in the first cycle can be correlated with the number of C–H bonds in the carbon, as shown in Fig. 11c. Such C–H bonds may be lost during cycling. Hence, some chemical reactions between lithium of lower valence and C–H bonds or edge carbon of the hexagonal planes, as described by Eqs. (1) and (2), may take place.

*Charge*

$$2Li^{\Delta+} + 2AR\text{-}\overset{H}{\underset{|}{|}} + 2\Delta e \longrightarrow 2AR\text{-}Li \quad (AR: \text{aromatic ring}) \tag{1}$$

*discharge*

$$2AR\text{-}\overset{H}{\underset{|}{|}} \longrightarrow 2Li^{+} + H_2 + 2AR + 2e$$

*charge*

$$Li^{\Delta+} + AR + \Delta e \rightarrow AR\text{-}Li$$

*discharge* (2)

$$2AR\text{-}Li \rightarrow 2Li^{+} + 2AR + 2e$$

Such AR-H should be paired at the edges of the two planes, being located in anisotropic carbons calcined at low temperatures. Some edges of hexagonal planes may not carry hydrogen (Eq. (2)) where they are located face-to-face in a short distance. Such reactions are irreversible to give a higher potential on discharge and reduce the capacity during subsequent cycles. Such a reaction is consistent with the valence of charged lithium measured by solid-state $^{7}$Li-NMR [5,16]. The difference between dischargeable and undischargeable sites is due to the completion of the reaction before or after the discharge. The distance between paired sites or the size of the aromatic ring may define the reactivity of such sites, as described below.

The correlation in Fig. 11c may provoke the question: why does the capacity of Type III decrease gradually according to the charge–discharge cycle if the capacity correlates with the H/C ratio? All the sites are not charged during one cycle over a limited period of the time. Hence, the value of H/C indicates the number of chargeable sites but not those that are charged during one cycle.

Higher temperature heat-treatment combines two edges of hexagonal planes with or without edge hydrogen into larger planes in the anisotropic carbon and enhances thick stacking into a more graphitic structure to reduce the voids, and hence the capacity, of this type. Fig. 13 illustrates the three types of insertion mechanisms into soft carbon heat-treated at 500 to 1200°C.

The conductivity is very much improved by higher temperature heat-treatment to reduce the overpotential and

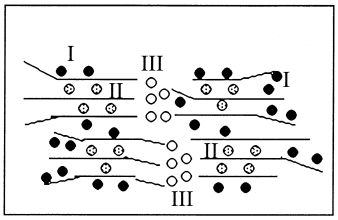


I : Hexagonal surface Li
II : Intercalated Li
III : Inserted into cluster gap
Type I : surface site
Type II : intercalation site ( higher stage )
Type III : orientation angle,
plane dimension or composition,
edge bonds

Fig. 13. Schematic model for lithium insertion into carbon heat-treated at low temperature.

discharge potential, although such voids are removed from the graphitizable carbon by such treatment. Disordered carbon can retain such voids up to a higher temperature of heat-treatment than the graphitizable carbon.

The last capacity is the undischargeable one, which is also observed during charging at a lower potential of about 0.1 V. The oxidation reactions of lithium of low valence as described in Eqs. (3) and (4) may take place:

$$2Li^{\Delta+} + 2AR\text{-}H + 2\Delta e \rightarrow 2AR + 2LiH \tag{3}$$

$$2Li^{\Delta+} + 2AR\text{-}OH + 2\Delta e \rightarrow AR\text{-}O\text{-}AR + Li_2O + H_2 \tag{4}$$

Carbons heat-treated at lower temperature carry more numbers of such reactive sites and, thereby, suffer more undischargeable charge.

The reaction of electrolyte on the carbon surface by the aid of low-valent lithium may also cause the undischargeable charge as reported in the graphite electrode. IR spectra of the anode after numbers of cycles indicates more organic products on the carbon anode calcined at 600°C than on that prepared at 1000°C, as shown in Fig. 14 [17]. The edges of the hexagonal plane may also participate into

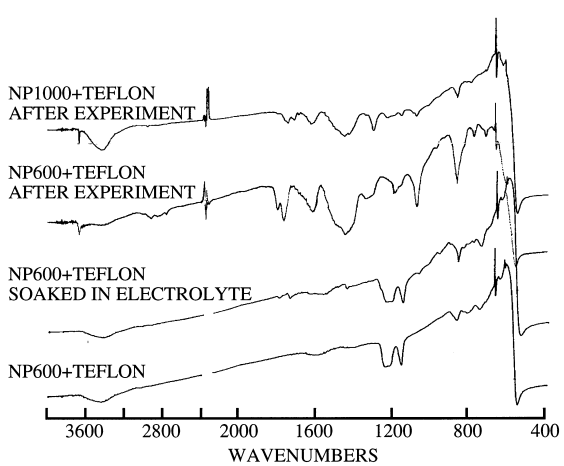


Fig. 14. FT-IR spectra of carbons prepared from NP mesophase pitch after 20 charge–discharge cycles. Constant-current charging method: 0.2 mA $cm^{-2}$; 0.0 to 2.0 V.

this kind of reaction. Surface modification has been reported to be effective [6,18,19].

## Acknowledgements

This study was supported by the Proposal-Based New Industry Creative Type Technology R&D Promotion Program from the New Energy and Industrial Technology Development Organization (NEDO) of Japan.

## References

[1] K. Sato, M. Noguchi, A. Demachi, N. Oki, M. Endo, Science 264 (1994) 556.
[2] J.R. Dahn, T. Zheng, Y. Liu, J.S. Xue, Science 270 (1995) 590.
[3] S. Yata, H. Kinoshita, M. Komori, N. Ando, T. Kashiwamura, T. Haradam, K. Tanaka, T. Yamabe, Synth. Metals 62 (1994) 153.
[4] W. Xing, J.S. Xue, J.R. Dahn, J. Electochem. Soc. 143 (1996) 3046.
[5] Y. Mori, T. Iriyama, T. Hashimoto, S. Yamazaki, F. Kawakami, H. Shiroki, T. Yambe, J. Power Sources 56 (1995) 205.
[6] J.S. Xue, J.R. Dahn, J. Electrochem. Soc. 142 (1995) 3668.
[7] T. Zheng, W. Xing, J.R. Dahn, Carbon 34 (1996) 1501.
[8] K. Tokumitsu, A. Mabuchi, H. Fujimoto, T. Kasuh, J. Electrochem. Soc. 143 (1996) 2235.
[9] J.R. Dahn, R. Fong, M.J. Spoon, Phys. Rev. B 42 (1990) 6424.
[10] J.R. Dahn, Phys. Rev. B 44 (1991) 9170.
[11] A. Mabuchi, K. Tokumitsu, H. Fujimoto, T. Kasuh, J. Electrochem. Soc. 142 (1995) 1041.
[12] Y. Liu, J.S. Xue, T. Zheng, J.R. Dahn, Carbon 34 (1996) 193.
[13] T. Zheng, W.R. McKinnon, J.R. Dahn, J. Electrochem. Soc. 143 (1996) 2137.
[14] Y. Matsumura, S. Wang, J. Mondori, Carbon 33 (1995) 1457.
[15] W. Xing, J.S. Xue, T. Zheng, A. Gibaud, J.R. Dahn, J. Electrochem. Soc. 143 (1996) 3482.
[16] K. Tatsumi, T. Akai, T. Imamura, K. Zaghib, N. Iwashita, S. Higuchi, Y. Sawada, J. Electrochem. Soc. 143 (1996) 1923.
[17] D. Aurbach, Y. eia-Eli, O. Chusid (Youngman), Y. Carmeli, M. Babai, H. Yamin, J. Electrochem. Soc. 141 (1994) 603.
[18] H. Fujimoto, A. Mabuchi, K. Tokumitsu, T. Kasuh, J. Power Sources 54 (1995) 440.
[19] R. Fong, U. bon Sacken, J.R. Dahn, J. Electrochem. Soc. 137 (1990) 2009.